JPNT 7(3), 175-181 (2018)
https://doi.org/10.11003/JPNT.2018.7.3.175

JPNT Journal of Positioning, Navigation, and Timing

Combined GPS/GLONASS Relative Receiver DCB Estimation Using the LSQ Method and Ionospheric TEC Changes over South Korea

Byung-Kyu Choi[1†], Ha Su Yoon[1], Sang Jeong Lee[2]

[1]Space Geodesy Group, Korea Astronomy and Space Science Institute, Daejeon 34055, Korea
[2]Department of Electronics Engineering, Chungnam National University, Daejeon 34134, Korea

ABSTRACT

The use of dual-frequency measurements from the Global Navigation Satellite System (GNSS) enables us to observe precise ionospheric total electron content (TEC). Currently, many GNSS reference stations in South Korea provide both GPS and GLONASS data. In the present study, we estimated the grid-based TEC values and relative receiver differential code biases (DCB) from a GNSS network operated by the Korea Astronomy and Space Science Institute. In addition, we compared the diurnal variations in a TEC time series from solutions of the GPS only, the GLONASS only, and combined GPS/GLONASS processing. A significant difference between the GPS only TEC and combined GPS/GLONASS TEC at a specific grid point over South Korea appeared near the solar terminator. It is noted that GLONASS measurements can contribute to observing a variation in ionospheric TEC over high latitude regions.

Keywords: GNSS, ionosphere, TEC, DCB

1. INTRODUCTION

The ionosphere affects all devices that use navigation signals such as a global navigation satellite system (GNSS), and acts as the largest error source during the signal transmission process from satellite to ground reference station. The GNSS signals are influenced by free electrons in the ionosphere when they pass through the ionosphere. The GNSS signals received at the ground contain various types of noises and receiver clock errors incur significant errors to determine relative signal delay in the navigation system that uses two frequencies.

Hofmann-Wellenhof et al. (1993) proposed the extraction of total electron content (TEC) from the global positioning system (GPS) signal delay. Since then, it has been utilized in various studies including a study on the TEC characteristics (Wilson & Mannucci 1993), a study on vertical distribution of electron density (Hajj et al. 1994), a study on the ionospheric irregularities (Wanninger et al. 1994), a study on sporadic E (Coco et al. 1995), a study on the detection of large-scale traveling ionospheric disturbances (LSTID) (Ho et al. 1996), and a study on the ionospheric disturbance (Calais & Minster 1998).

As the number of GNSS reference stations that receive GLObal NAvigation Satellite System (GLONASS) signals increases, studies on the ionosphere using GLONASS along with GPS tend to increase as well. Camargo (2009) calculated the receiver's inter-frequency bias and vertical TEC using the GPS/GLONASS data observed by three types of GNSS receivers (Topcon TPS Hyper, Trimble NetR5, and Leica GRX1200) to analyze the errors given to L1 frequency signals. Afraimovich et al. (2013) reported that the problems of global ionospheric disturbance detection along with a spatial resolution that could not be solved by GPS/GLONASS previously were able to be resolved. Zakharenkova et al. (2016) published a paper that can reveal the results of the spatiotemporal resolution in the ionosphere. They were able to analyze the radio properties of LSTID using GPS and GLONASS measurements received at around 5,300 reference stations during the St. Patrick's day storm from March 17 to 18 in 2015. Nakashima & Heki (2014) employed

Received June 26, 2018 **Revised** July 03, 2018 **Accepted** July 13, 2018
†**Corresponding Author**
E-mail: bkchoi@kasi.re.kr
Tel: +82-42-865-3237 Fax: +82-42-861-5610

GPS observations to analyze the rocket-induced ionospheric disturbance after a rocket launch. However, the rocket-induced ionospheric disturbance was not detected due to the geometric problem of GPS satellites. Therefore, they used GLONASS data to overcome this problem. In addition, Yasyukevich et al. (2015) determined the ionospheric TEC using the GPS and GLONASS measurements. They developed an algorithm that can estimate differential code biases (DCBs) based on a single GNSS reference station. They also proposed that 1 ns DCB value led to ~ 2.9 TEC unit (TECU) error when determining the TEC with the GPS dual frequency.

The utilization of GLONASS along with GPS has increased steadily to analyze the TEC in the ionosphere. This study employed the data received in every 30 sec from nine GNSS reference stations operated by the Korea Astronomy and Space Science Institute to calculate GPS/GLONASS TEC over the Korean Peninsula. In addition, the GNSS receiver DCBs that are the largest error source in the ionospheric TEC calculation are calculated relatively by applying the least square (LSQ) method, and the characteristics of GPS and GLONASS receiver DCBs are analyzed respectively. Furthermore, the TEC values over the Korean Peninsula calculated with other data processing methods are compared and analyzed.

2. DATA PROCESSING METHOD

2.1 TEC Calculation

The GPS satellites broadcast two carrier frequencies in the L-band (L1 = 1575.42 MHz and L2 = 1227.60 MHz) to the ground. The reception of dual frequency of the GLONASS satellites at the ground can determine the positioning of users as well as calculate the ionospheric TEC value accurately in contrast with GPS signals. The ionospheric error that acts as the largest error in the navigation signal transmission process can be eliminated through the widely known "ionosphere-free linear combination". On the other hand, "geometry-free linear combination" is used for estimating the ionospheric error accurately, which has been introduced in a number of studies (Davies & Hartmann 1997, Calais & Minster 1998, Mannucci et al. 1999, Afraimovich et al. 2001, and Otsuka et al. 2002). This study employed a method proposed by Sardon et al. (1994).

$$STEC = \frac{1}{40.3}\left(\frac{f_1^2 \cdot f_2^2}{f_1^2 - f_2^2}\right) \times [(L_1 - L_2) - (\lambda_1 N_1 - \lambda_2 N_2) + b_r + b^s] \quad (1)$$

where, f_1 and f_2 refer to frequencies of the GNSS navigation signals. In the case of GPS, f_1 and f_2 are 1575.42 MHz and 1227.60 MHz, respectively. However, GLONASS uses a frequency division method so the two frequencies are determined to f_1 = (1602+k·0.5625) MHz and f_2 = (1246+k·0.4375) MHz, respectively. In the above frequencies, k refers to a frequency channel number. The channel number k of the GLONASS satellite can be checked in the satellite navigation file. L_1 and L_2 refer to carrier phase measurements of the GLSS L1 and L2. λ_1 and λ_2 refer to the wavelengths of the two frequencies. N_1 and N_2 refer to the integer ambiguity. b_r and b^s are DCBs of the GNSS receiver and satellite. STEC refers to slant TEC, which is a measurement of the ionospheric TEC in the line of sight direction between the navigation satellite and receiver. We assume that free electrons are concentrated at a fixed height to estimate the TEC from the GNSS. Although the shell height is different from ionospheric models, it is generally set within a range of 250 km - 450 km. In this study, it was assumed as 300 km (Otsuka et al. 2013).

Since *STEC* significantly varies depending on a satellite elevation, a conversion of *STEC* into vertical TEC (VTEC) is conducted. As presented in Eqs. (2) and (3), a mapping function is needed to convert *STEC* into *VTEC*. In this study, "a modified single layer mapping function" proposed by Grejner-Brzezinska et al. (2004) was used.

$$VTEC = STEC / M(z) \quad (2)$$

$$M(z) = \frac{1}{\cos(z')}, \ \sin(z') = \frac{R_E}{R_E + h}\sin(\alpha \cdot z) \quad (3)$$

where, M is a mapping function, z and z' refer to the receiver's location and zenith angle at the ionospheric pierce point (IPP), respectively. R_E is the radius (6,371 km) of the earth, and h refers to a height assumed where the TEC is the most concentrated (300 km) at the ionosphere. In addition, α is a correction factor (0.9872).

In this study, we set the elevation angle of the GNSS satellite to 20° to reduce the effect of a multi-path error.

2.2 GPS/GLONASS Relative Receiver DCB Estimation

One of the largest factors that decrease the accuracy of the GNSS TEC is the hardware bias derived from the GNSS receivers and satellites (Lanyi & Roth 1988). The GNSS TEC is calculated by the geometry-free linear combination. That is, a hardware bias is included in the observation of different frequencies, and a difference of measurements is used to calculate the ionospheric TEC. The hardware bias that is included in each of the frequencies has a differential form, which is a DCB. Every GNSS receiver has different characteristics of DCB which can reach up to nanoseconds

https://doi.org/10.11003/JPNT.2018.7.3.175

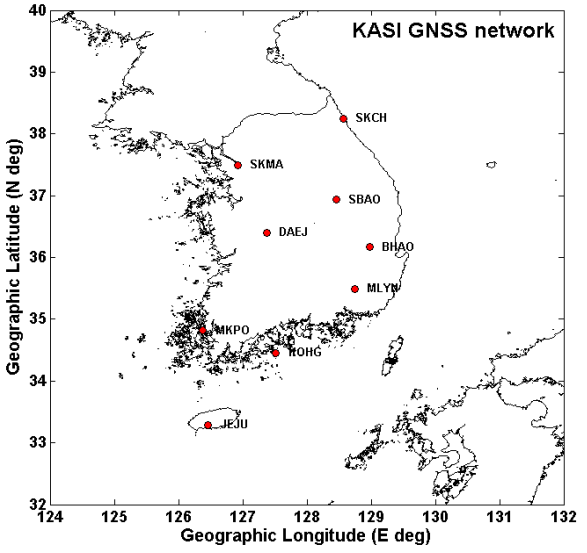

Fig. 1. The distribution of the GNSS reference stations in this study. Red filled circles indicate the location of GNSS sites.

(ns). The DCB of the GNSS satellites is somewhat smaller than that of the receiver but it also has the value up to several ns. Thus, DCBs that are created by the GNSS satellites and receivers must be calculated and removed from the observed value to calculate the ionospheric TEC precisely.

In this study, an algorithm was developed to determine the DCBs of GPS and GLONASS receivers simultaneously as presented in Eq. (4).

$$\begin{bmatrix} \cdots & 0 & 0 & 0 & 0 & 0 & 0 & 0 & 0 \\ \cdots & 0 & 0 & 0 & 0 & 0 & 0 & 0 & 0 \\ \cdots & \vdots & \vdots & \vdots & \vdots & \vdots & \vdots & \vdots & \vdots \\ M_{G1} \cdots 0\ 1\ 0 & \vdots & \vdots & \vdots & \vdots & \vdots & \vdots & \vdots & \vdots \\ \cdots & \vdots & \vdots & \vdots & \vdots & \vdots & \vdots & \vdots & \vdots \\ M_{Gi} \cdots 1\ 0 & 0 & 0 & 0 & 0 & 0 & 0 & 0 & 0 \\ 0\ 0\ 0\ 0\ 0\ 0\ 0\ 0\ 0\ 0 \cdots & \cdots & & & & & & & \\ 0\ 0\ 0\ 0\ 0\ 0\ 0\ 0\ 0\ 0 \cdots M_{R1} \cdots & 0\ 1 & \cdots & 0 & & & & & \\ \vdots\ \vdots\ \vdots\ \vdots\ \vdots\ \vdots\ \vdots\ \vdots\ \vdots\ \vdots \cdots & \cdots & & & & & & & \\ \vdots\ \vdots\ \vdots\ \vdots\ \vdots\ \vdots\ \vdots\ \vdots\ \vdots\ \vdots \cdots M_{Rj} & 0 & \cdots & 1 & & & & & \\ 0\ 0\ 0\ 0\ 0\ 0\ 0\ 0\ 0\ 0 \cdots & \cdots & & & & & & & \end{bmatrix} \begin{bmatrix} VTEC_{G1} \\ \vdots \\ VTEC_{Gi} \\ b_{rG1} \\ \vdots \\ b_{rGk} \\ VTEC_{R1} \\ \vdots \\ VTEC_{Rj} \\ b_{rR1} \\ \vdots \\ b_{rRk} \end{bmatrix} = \begin{bmatrix} STEC_{G1} \\ \vdots \\ STEC_{Gi} \\ STEC_{R1} \\ \vdots \\ STEC_{Rj} \end{bmatrix} \quad (4)$$

where, G and R refer to GPS and GLONASS, and subscript k refers to the GNSS reference stations.

Each GPS and GLONASS receiver DCB is estimated relatively as the DCB of the DAEJ GNSS reference station is set as "Reference". GPS C1-P2 DCB and GLONASS P1-P2 DCB for the receiver in the DAEJ reference station employed a value of Global Ionosphere Map product provided by the Natural Resources Canada. The information on satellite C1-P1 DCB and P1-P2 DCB values is obtained from the Center for Orbit Determination in Europe (CODE) in Switzerland in case of GPS and GLONASS satellites. The CODE generates and provides satellite DCB files in the form of C1P1yymm.DCB.Z and P1P2yymm.DCB.Z. In this study, satellite DCB values are not estimated separately but employed the information calculated from the CODE Analysis Center.

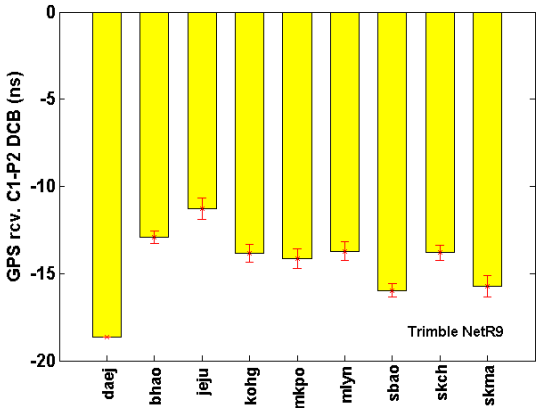

Fig. 2. The estimated C1-P2 DCB values for GPS receivers in KGN on November 1, 2017.

3. RESULTS AND ANALYSIS

3.1 Analysis on GPS and GLONASS Receiver DCB

The data obtained in the permanent GNSS observation network operated by the Korea Astronomy and Space Science Institute were used to calculate the ionospheric TEC. The Korea Astronomy and Space Science Institute operates a total of nine GNSS reference stations in Korea. Fig. 1 shows the locations of the GNSS reference stations. The Trimble NetR9 receiver and TRM59800.00 type of antennas are installed in all reference stations.

Fig. 2 shows the daily GPS C1-P2 DCBs in each reference station calculated using the observation data on Nov. 1 in 2017. The receiver DCBs at each reference station are calculated every hour and a mean value for 24 hours is calculated. The yellow bar graph in Fig. 1 indicates the receiver DCBs, respectively. The red error bar indicates the standard deviation. The GPS receiver C1-P2 DCB has a range of -12 ns to -18 ns, and JEJU Reference Station has a maximum value as -12 ns, and DAEJ Reference Station has a minimum value as -18 ns. Despite that the same type of receiver Trimble NetR9 was employed, all receiver C1-P2 DCBs were calculated differently. The receiver DCB is known to be affected by the GNSS data quality, DCB estimation method, characteristics of receiver and antenna, and internal hardware temperature of the receiver (Warnaut 1997, Coster et al. 2013). Zhang et al. (2009) also reported that the receiver DCBs differed according to the geomagnetic condition. More recently, Choi & Lee (2018) published that the receiver DCB was significantly affected by antenna grounding in the reference station. The various factors suggested in the above

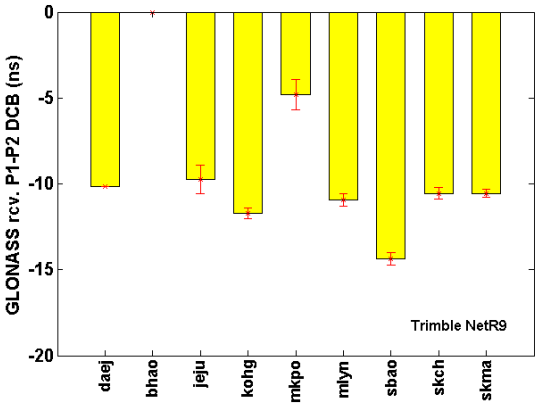

Fig. 3. The estimated P1-P2 DCB values for GLONASS receivers in KGN on November 1, 2017.

may have affected the receiver DCB in Fig. 2 complexly as well.

Fig. 3 shows the daily GLONASS receiver P1-P2 DCB in each reference station processed in the same period. The GLONASS receiver P1-P2 DCB is marked as the yellow bar graph, and the standard deviation of the DCBs is indicated as the red error bar. The GLONASS P1-P2 DCBs have a range of -5 ns to -15 ns, in which a difference between the maximum and minimum values is relatively larger than that of GPS C1-P2 DCB. The GLONASS receiver DCB has approximately the maximum value of -5 ns in MKPO Reference Station, and the minimum value of -15 ns in SBAO Reference Station. These values show different characteristics by reference stations. It is difficult to find a common factor between the GPS receiver DCB in Fig. 2 and GLONASS receiver DCB in Fig. 3 from the reference station viewpoint. Note that the absolute values of GPS and GLONASS receiver DCBs in SBAO Reference Station were slightly larger than those of other reference stations in a relative aspect. It is not easy to find a factor in this cause. However, given that the same type of GNSS receivers, same antennas, and the same cables were used, the grounding conditions around the reference stations as reported by Choi & Lee (2018) may affect the receiver DCBs. In addition, BHAO Reference Station DCB was calculated to 0 ns, which was due to abnormal data processing as a result of the absence of the GLONASS P1 code measurements during the same period.

3.2 Analysis on the Change in the GNSS Ionospheric TEC over the Korean Peninsula

The GPS and GLONASS observation data were employed simultaneously to monitor the change in the ionospheric TEC precisely over the Korean Peninsula. Fig. 4 shows the IPP of GPS and GLONASS satellite signals according to the latitude and longitude. Fig. 4a shows the change in IPP for two hours

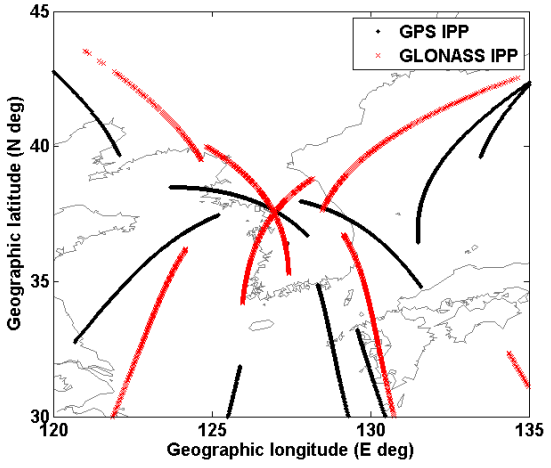

(a) 2 hours

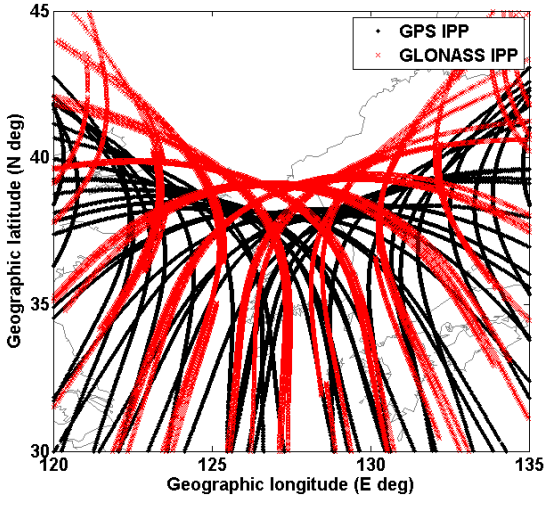

(b) 24 hours

Fig. 4. IPP tracks for GPS and GLONASS satellites observed from daej site on November 1, 2017: (a) for 2 hours (03:00 – 05:00 UT), (b) for 24 hours.

(03:00 – 05:00 UT) based on DAEJ Reference Station, in which the black dotted line refers to the IPP of GPS satellite, and the red cross marker refers to the IPP of the GLONASS satellite. As shown in Fig. 4a, when GPS satellite as well as the GLONASS satellite are added, the advantages of the GLONASS use are well displayed. That is, some regions that cannot be observed by GPS satellite at a specific time can be well covered by the GLONASS satellite. Fig. 4b shows the change in IPP of GPS and GLONASS satellites in a day. The overall characteristic of the IPP distribution revealed that the IPP in the GLONASS satellite was more distributed in the northern region in the Korean Peninsula than that of the GPS satellite. This is related to the inclination angle of the satellites. The orbital inclination angles of GPS and GLONASS satellites are 55° and 64.8°, respectively. That is, since the orbital inclination angle of the GLONASS satellite is larger than that of the

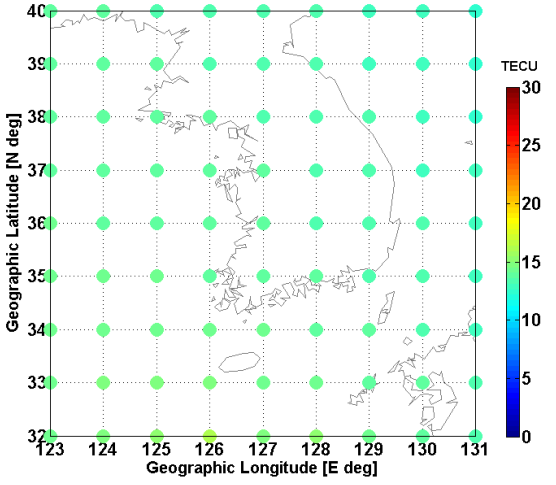

Fig. 5. Grid TEC maps over South Korea derived from inverse distance weighted interpolation method.

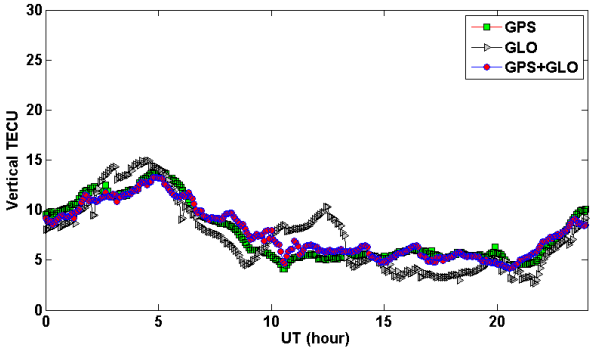

Fig. 6. Comparison of the diurnal TEC changes at a specific grid point (36° N, 127° E) on November 1, 2017. The green squares and gray right-pointing triangles indicate TEC values obtained from GPS only, GLONASS ('GLO') only, respectively. The red circles show TEC changes calculated from combined GPS+GLO system.

GPS satellite, the IPP distribution of the GLONASS satellite is positioned farther to the north direction than that of the GPS satellite. Thus, GLONASS plays a very important role in monitoring the changes in the ionospheric TEC in the northern sky of the Korean Peninsula. In particular, the use of GLONASS plays a significant role in analyzing the ionosphere in high latitude areas such as polar regions.

This study calculated the ionospheric TEC by dividing the data utilization method into GPS only, GLONASS ('GLO') only, and the GPS+GLO combination, and then recalculated the grid-based ionospheric TEC as shown in Fig. 5 utilizing the inverse distance weighted interpolation technique. The VTEC at a specific grid point (36° N, 127° E) over the Korean Peninsula was calculated to compare the change in TEC according to the different data utilization method, which is shown in Fig. 6 in a time-series form. In Fig. 6, the daily

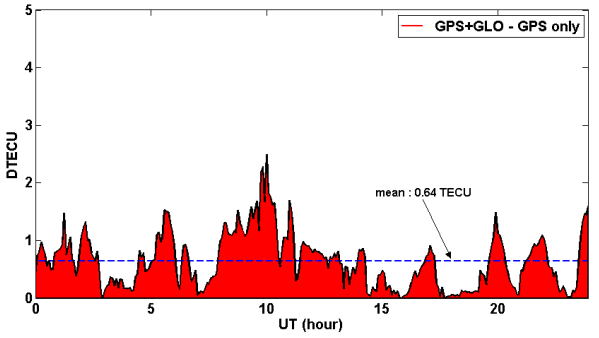

Fig. 7. TEC difference between GPS only and GPS+GLONASS on November 1, 2017. The blue dot line indicates an average value for ionospheric TEC differences for that day.

changes in the TEC according to GPS only, GLO only, and the GPS+GLO combination are marked as green squares, gray right-pointing triangles, and red circles, respectively. The daily changes in the three TECs were similar to one another. The time when the VTEC was at the maximum was approximately 5:00 UT and changes in VTEC for about ten hours (10:00 - 20:00 UT) from the dusk to the dawn was five to seven TEC units (TECU), which was highly stable. In contrast, GLO TEC had a difference up to 5 TECU at a specific time compared to those of GPS TEC and GPS+GLO TEC. Since the number of satellites in the case of GLO was relatively smaller than that of the GPS, larger errors may occur when generating the grid-based TEC. On the other hand, a change in TEC due to GPS+GLO was nearly similar to that of the GPS only TEC.

Fig. 7 shows the difference between GPS only TEC and GPS+GLO TEC displayed in Fig. 6 by the time change. The difference in TEC between the two methods was approximately 0.64 TECU daily on average, which is marked as the blue dotted line in Fig. 7. Considering the standard deviation and observation noise of the GNSS receiver DCB, there seemed to be few differences in TEC between two methods. However, the difference between the two methods at approximately 10:00 UT, which was the solar terminator time, reached up to 2.5 TECU. The change in the ionospheric TEC has been known to be the largest at the solar terminator. Cot & Teitelbaum (1980) reported that the movement of the solar terminator generated the acoustic-gravity waves, and induced the disturbance of the ionospheric plasma. As shown in Fig. 6, considering that the background TEC was approximately seven TECU at 10:00 UT, the difference in TEC at that time reached approximately 35%. It is necessary to analyze the reasons for the difference for a long-term basis whether such difference is due to the use of GLONASS measurements, changes in receiver DCBs, and characteristics of changes in the ionosphere itself, or complex effects of the above.

4. CONCLUSIONS

This study analyzed the changes in the ionospheric TEC utilizing the data of GPS and GLONASS received on Nov. 1 in 2017 from the GNSS reference stations operated by the Korea Astronomy and Space Science Institute. The receiver DCB, which acted as the largest error in calculating the ionospheric TEC accurately, was determined relatively. When the same type of Trimble NetR9 receiver and TRM59800.00 antenna were used at nine GNSS reference stations, GPS receiver C1-P2 DCB was in a range of -12 ns to -18 ns, and the GLONASS receiver P1-P2 DCB was in a range of -5 ns to -15 ns. That is, receiver DCBs were calculated differently in the GNSS reference stations. The large difference in DCBs among reference stations was due to the effect of antenna grounding reported by Choi & Lee (2018) although there were many various factors that affected the receiver DCBs.

The GPS and GLONASS IPP trajectory was analyzed to determine the effect of the GLONASS TEC over the Korean Peninsula. When the GPS signals are not observed in a short period of time, the GLONASS measurements can play a role in almost TEC estimation system. The GLONASS satellites have also larger orbit inclination than that of the GPS satellite as shown in the daily IPP analysis results. Therefore, IPP distribution in the GLONASS is located farther to the north direction in the Korean Peninsula than that of the GPS, thereby analyzing the changes in the ionospheric TEC in the northern region of the Korean Peninsula more accurately.

The daily changes in the ionospheric TEC were also compared and analyzed at a specific grid point (36° N, 127° E). The analysis results showed that a difference between GPS only TEC and GPS+GLO TEC was 0.64 TECU on average, which verified a highly similar characteristic of the change. However, a difference of approximately 2.5 TECU was revealed at a specific time such as the solar terminator between two different data processing methods. The reason for this requires further analysis on a long-term basis.

ACKNOWLEDGMENTS

This study was supported by the 2018 Primary Project of the Korea Astronomy and Space Science Institute (project: Operation of the Space Geodetic Infra-facilities and Research on Astronomical Almanac).

REFERENCES

Afraimovich, E. L., Astafyeva, E. I., Demyanov, V. V., Edemskiy, I. K., Gavrilyuk, N. S., et al. 2013, A review of GPS/GLONASS studies of the ionospheric response to natural and anthropogenic processes and phenomena, J. Space Weather Space Clim, 3, A27. https://doi.org/10.1051/swsc/2013049

Afraimovich, E. L., Kosogorov, E. A., Lesyuta, O. S., Ushakov, I. I., & Yakovets, A. F. 2001, Geomagnetic control of the spectrum of traveling ionospheric disturbances based on data from a global GPS network, Ann. Geophys., 19, 723-731

Calais, E. & Minster, J. B. 1998, GPS, earthquakes, the ionosphere, and the space shuttle, Phys. Earth Planet Inter, 105, 167-181. https://doi.org/10.1016/S0031-9201(97)00089-7

Camargo, P. O. 2009, Quality of TEC Estimated with Mod Ion Using GPS and GLONASS Data, Mathematical Problems in Engineering, Article ID 794578, 1-16. https://doi.org/10.1155/2009/794578

Choi, B. K. & Lee, S. J. 2018, The influence of grounding on GPS receiver differential code biases, ASR, 62, 457-463. https://doi.org/10.1016/j.asr.2018.04.033

Coco, D. S., Gaussiran, T. L., & Coker, C. 1995, Passive detection of sporadic E using GPS phase measurements, Radio Sci., 30, 1869-1874. https://doi.org/10.1029/95RS02453

Coster, A., Williams, J., Weatherwax, A., Rideout, W., & Herne, D. 2013, Accuracy of GPS total electron content: GPS receiver bias temperature dependence, Radio Sci., 48, 190-196. https://doi.org/10.1002/rds.20011

Cot, C. & Teitelbaum, H. 1980, Generation of gravity waves by inhomogeneous heating of the atmosphere, J. Atmos. Terr. Phys., 42, 877-883. https://doi.org/10.1016/0021-9169(80)90092-6

Davies, K. & Hartmann, G. K. 1997, Studying the ionosphere with the Global Positioning System, Radio Sci., 32, 1695-1703. https://doi.org/10.1029/97RS00451

Grejner-Brzezinska, D. A., Wielgosz, P., Kashani, I., Smith, D. A., Spencer, P. S. J., et al. 2004, An analysis of the effects of different network-based ionosphere estimation models on rover positioning accuracy, Journal of GPS, 3, 115-131. https://doi.org/10.5081/jgps.3.1.115

Hajj, G. A., Ibanez-Meier, R., Kursinski, E. R., & Romans, L. J. 1994, Imaging the ionosphere with the global positioning system, International Journal of Imaging Systems and Technology, 5, 174-187. https://doi.org/10.1002/ima.1850050214

Ho, C. M., Mannucci, A. J., Lindqwister, U. J., Pi, X., & Tsurutani, B. T. 1996, Global ionospheric Perturbations monitored by the worldwide GPS network, Geophys. Res. Lett., 23, 3219-3222. https://doi.org/10.1029/96GL02763

Hofmann-Wellenhof, B., Lichtenegger, H., & Collins, J. 1993,

Global Positioning System: Theory and Practice, 2nd ed. (New York: Springer-Verlag)

Lanyi, G. E. & Roth, T. 1988, A comparison of mapped and measured total ionospheric electron content using global positioning system and beacon satellite observation, Radio Sci., 23, 483-492. https://doi.org/10.1029/RS023i004p00483

Mannucci, A., Iijima, B., Sparks, L., Pi, X., Wilson, B., et al. 1999, Assessment of global TEC mapping using a three-dimensional electron density model, J Atmos. Sol. Terr. Phys., 61, 1227-1236. https://doi.org/10.1016/S1364-6826(99)00053-X

Nakashima, Y. & Heki, K. 2014, Ionospheric hole made by the 2012 North Korean rocket observed with a dense GNSS array in Japan, Radio Sci., 49, 497-505. https://doi.org/10.1002/2014RS005413

Otsuka, Y., Ogawa, T., Saito, A., Tsugawa, T., Fukao, S., et al. 2002, A new technique for mapping of total electron content using GPS network in Japan, Earth, Planets and Space, 54, 63-70. https://doi.org/10.1186/BF03352422

Otsuka, Y., Suzuki, K., Nakagawa, S., Nishioka, M., Shiokawa, K., et al. 2013, GPS observations of medium-scale traveling ionospheric disturbances over Europe, Ann. Geophys., 31, 163-172. https://doi.org/10.5194/angeo-31-163-2013

Sardon, E., Rius, A., & Zarraoa, N. 1994, Estimation of the transmitter and receiver differential biases and the ionospheric total electron content from Global Positioning System observations, Radio Sci., 29, 577-586. https://doi.org/10.1029/94RS00449

Wanninger, L., Sardon, E., & Warnant, R. 1994, Determination of the total ionospheric electron content with GPS-Difficulties and their solution, Proceedings of Beacon Satellite Symposium '94, ed. L. Kersley (Aberystwyth: Univ. of Aberystwyth), pp.13-16. http://hdl.handle.net/2268/84763

Warnant, R. 1997, Reliability of the TEC computed using GPS measurements - The problem of hardware biases, Acta Geod. Geophys. Hung., 32, 451-459

Wilson, B. D. & Mannucci, A. J. 1993, Instrumental biases in ionospheric measurements derived from GPS data, in ION GPS 1993 (Institute of Navigation), September 22-24, 1993, Salt Palace Convention Center, Salt Lake City, UT, pp.1343-1351

Yasyukevich, Y. Y., Mylnikova, A. A., & Polyakova, A. S. 2015, Estimating the total electron content absolute value from the GPS/GLONASS data, Results in Physics, 5, 32-33. https://doi.org/10.1016/j.rinp.2014.12.006

Zakharenkova, I, Astafyeva, E., & Cherniak, I. 2016, GPS and GLONASS observations of large-scale traveling ionospheric disturbances during the 2015 St. Patrick's Day storm, J. Geophys. Res. Space Physics, 121, 12138-12156. https://doi.org/10.1002/2016JA023332

Zhang, W., Zhang, D. H., & Xiao, Z. 2009, The influence of geomagnetic storms on the estimation of GPS instrumental biases, Ann. Geophys., 27, 1613-1623. https://doi.org/10.5194/angeo-27-1613-2009

Byung-Kyu Choi received the Doctor's degree in Electronics in Chungnam National University in 2009. He has been working at the Korea Astronomy and Space Science Institute since 2004. His research interests include multi-GNSS PPP, PPP-RTK and GNSS TEC modeling.

Ha Su Yoon received a Ph.D. degree in Department of Geoinformatics in University of Seoul in 2015. Since 2016, he has been with the Korea Astronomy and Space Science Institute. His current research interests include GNSS meteorology and Ocean tide Loading.

Sang Jeong Lee received the Doctor's degree in Control and Measurement in Seoul National University in 1987. His research interests include GNSS and Robust Control.